Journal of Sound and Vibration (2002) **254**(1), 1–21
doi:10.1006/jsvi.2001.4052 available online at http://www.idealibrary.com on IDEAL®

LINING-DEFORMATION-INDUCED MODAL COUPLING AS SQUEAL GENERATOR IN A DISTRIBUTED PARAMETER DISC BRAKE MODEL

J. FLINT

Institute of Applied Physics, University of Southern Denmark, Niels Bohrs Allé 1, *DK*-5230 *Odense, Denmark*

AND

J. HULTÉN

Volvo Truck Corporation, SE-405 08 *Göteborg, Sweden*

(*Received* 29 *September* 2000, *and in final form* 23 *August* 2001)

A distributed-parameter model of a disc brake is developed, which is used for simulation of friction-induced vibrations in the form of high-frequency squeal. The effect of different squeal generation mechanisms is investigated. The comparison of measured and calculated frequencies shows a good agreement and this study indicates that lining-deformation-induced modal coupling can act as a squeal generator in disc brakes.

1. INTRODUCTION

Being exposed to brake squeal can be very annoying and avoiding this problem has a high priority. Often considerable effort is needed in order to address squeal noise issues for the purpose of development, testing and implementation of vehicle brake systems.

High-frequency squeal from disc brakes is a difficult subject partly because of its fugitive nature and partly because the mechanical interactions in the friction disc brake is highly complicated. A multitude of different simplifications and interpretations have been suggested. At the moment no sufficiently accurate model or generally accepted understanding of the problem exists. It is the object of this study to investigate some basic mechanisms that may be involved in the generation of disc brake squeal and to make a simple, yet qualitatively correct model.

1.1. PREVIOUS WORK

A comprehensive review of the scientific work in the field of friction excited vibration was done by Ibrahim [1,2]. The following short review will focus on the types of mechanisms that various authors have used, in their effort to simulate disc brake squeal.

1.1.1. *Stick–slip and friction–velocity slope*

Basford and Twiss [3] described measurements of friction at low speed and concluded that "stick–slip friction ... cannot be responsible for vibration during high-speed

0022-460X/02/$35.00

operation of brakes''. In the accompanying article [4], a model for tangential vibration excited by stick–slip is formulated and the shear-modulus and the friction characteristic value $d\mu/dv$ is seen as the main factors influencing vibration.

Bannerjee [5] analyzed a mass sliding on a baseplate and established the critical velocity (in the area of 6–30 cm/s) above which no stick–slip will occur. This was done using a second order polynomial assumption of the friction–velocity relation. Brommundt [6] analyzed a three degree of freedom (3-d.o.f.) model of a two-mass system on a moving belt. Even under the condition of monotonically increasing friction, the system can enter an unstable state of oscillation for given system parameter values. As the essential condition for instability, Brommundt refers to the coupling between degrees of freedom and the existence of inertial forces parallel and perpendicular to the rubbing surfaces.

Friction is known to vary not only with speed, but also with temperature, pressure, time history, etc. An interesting investigation on friction–temperature constitutive laws governing the friction of rosin has been carried out by Smith and Woodhouse [7].

1.1.2. *Sprag-slip or kinematic constraint instability models*

Spurr [8] investigated occurrences of squeal in railway, drum and disc brakes under different service conditions. These observations as well as experiments on a rotating telephone bell preceded the presentation of a simple model, where a pin in sliding contact with a moving plane begins to ''spragge'' under certain angles of attack. A state of oscillation was possible provided the angle θ between the pin and the plane was approaching

$$\mu = \cot\theta. \tag{1}$$

So this model linked the magnitude of the friction coefficient and the position of the point of contact of the friction pad and its support directly to the occurrence of squeal. In a later paper [9], Spurr gave the following description of the phenomenon: ''...during squeal the friction material is deflected elastically along the disc surface by the frictional force. This deflection causes a second deflection with a component normal to the surface of the pad which reduces the friction and the stored elastic energy returns the system to the first configuration, and the cycle is repeated. The phase difference between the two coupled vibrations necessary to maintain oscillation arises from the intertias of the system.''

An extensive theoretical analysis is presented by Jarvis and Mills [10]. A pin-on-disc experiment was conducted and the configuration was modelled with two modes on the disc for any resonant frequency. The appendix of that paper explains in detail how such two modes can be combined to represent any wave motion, stationary and travelling. Even though correlation between experiment and theoretical prediction was poor, two main conclusions were drawn from the analysis: ''The variation of coefficient of friction was not responsible for the maintenance of the vibration''... ''The instability is due to the type of coupling between the two components and depends on the geometric configuration.'' These findings—though not entirely new—had considerable influence on subsequent researchers.

Earles and co-workers described in many papers experimental and analytical work related to brake squeal. In reference [11], an experimental setup was described consisting of a pin a disc. The pin had a translational and a rotational d.o.f. and was arranged in an angle of inclination φ to the disc. This angle is related to the angle θ in equation (1) by $\varphi = \pi/2 - \theta$, and if this angle was in the range

$$\arctan\mu > \varphi > 0, \tag{2}$$

an unstable oscillatory motion could be experienced for certain system parameters. Two mathematical models for translational and rotational modes, respectively, predicted the

torsional mode to be the one with exponentially growing amplitude. The model predicted a stable limit cycle to change into an unstable motion for the parameter values exceeding some limits. The torsional mode of the pin was associated with a "digging-in" action that could occur within the limits described by equation (2). In a subsequent paper [12], a parallel was drawn between the "sprag-slip" model of Spurr and a coupled model including modes of the pin and the disc. This model predicted the occurrences of the squeal near the free disc anti-resonance point. Later Earles and Badi [13] presented a two-pin-disc system. A second pin was applied to the other disc face. This system had 7 d.o.f. and two constraint equations. As the vertical motion was uncoupled, only 3 d.o.f. remained in the equation of motion. The relation represented by equation (2) no longer described the boundaries for instability, as the two pins could be arranged to enhance or counteract each others squeal generating action.

Busby *et al.* [14] reworked the 3-d.o.f. model developed by Earles and Badi [13]. By eigenvalue analysis as well as by transient time-domain analysis they worked with a linear as wall as a non-linear model. They used among other criteria an energy criterion, to describe the stability of the transient model.

Millner [15] analyzed a 5-d.o.f. model with a disc, one pad and one caliper part and a kinematic constraint securing contact between pad and disc. The main focus of the analysis was the location of the point of contact between pad and caliper. Ranges of instable behavior for the different parameters was given and the friction coefficient, caliper mass and stiffness was seen as the most important parameters.

Murakami *et al.* [16] developed a model where a kinematic constrained instability as well as a falling μ-velocity characteristic was responsible for the disc brake squeal. The 7-d.o.f. model allowed the rigid disc to have a rotational d.o.f. and the pads to rotate as well as translate in the in-plane direction. The squeal generation mechanism was attributed to the coupled vibration of the system, with squeal energy source stemming from the μ-velocity characteristics and from the moment on the pad generated by the offset of the friction force and the abutment reaction force.

Nishiwaki [17] proposed a generalized theory of brake noise covering drum brake squeal, disc brake squeal and groan. The theory is based on dynamic instabilities of the brake system caused by friction force variations. "The amount of work of vibration of brake structures often differs between the forward and backward vibration motions, resulting in dynamic instability of the system...".

1.1.3. *Binary flutter*

The presence of two disc modes of vibration at the same frequency was an important fact as the basis for the work by North [18–20]. An 8-d.o.f. model of a disc brake was developed. A rigid bar representing the disc had a translational and a rotational d.o.f. These d.o.f. are representing a cosine and a sine vibration of the disc. In reference [20], a simplified 2-d.o.f. model representing the basic features of the 8-d.o.f. model is described and a criterion for oscillatory instability was established.

The mechanism responsible for the instability is described as binary flutter of two disc modes and "the theory ... relies only on the presence of the disc and the friction forces produced by pressure of elastic friction material". As the eventual verification of the theory, North pointed to the "detailed measurement of the modes of the squealing disc, including timephase and circumferential phase ..." [20].

Brooks *et al.* [21, 22] present a 12-d.o.f. model of a caliper with four opposed pistons. The pistons all have one translational d.o.f. the disc has one translational and one rotational d.o.f., while the pads have two translational and one rotational d.o.f. An

eigenvalue analysis is supplemented by a sensitivity analysis to establish, which parameters are most effective in influencing the instability level. The length of the pads, as well as the location of the point of contact between caliper and pad backplate, are some of the important parameters, while the damping parameters are said to be having a negligible effect on the location of the eignevalues in the complex plane.

Yuan [23] describes the formulation of a model, where the pads and rotor are made up of finite beam elements while the caliper is a rigid 2-d.o.f. component. The friction coefficient is assumed to be linearly dependent on the relative sliding speed. According to this study, coupled vibrations may exist even if the μ-velocity slope is not negative, but if $d\mu/dv < 0$ it will add to the squeal propensity. It was also concluded that "for certain brakes, the negative μ-velocity slope may have a dominant influence on squeal propensity".

1.1.4. *Follower forces*

Forces that change their directions as the geometry changes are called follower forces. Friction forces are always parallel to the surface and a rotation of a disc segment will result in a transverse component of the friction force. Such follower forces are non-conservative and can result in instabilities.

In a series of articles, Mottershead and co-workers have treated the effect of follower forces in the context of disc brake squeal. In reference [24], a finite element model of a disc brake is presented. The work was described as an extension of the work by North [20] and Millner [15], but here the excitation mechanism is formulated as a follower force type loading. The instability is termed "flutter" and it "... occurs when, with increasing magnitude of a parameter ... , two normal modes coalesce at a critical frequency."

A study of the effects of follower forces using multiple scales analysis is presented in reference [25]. An annular plate fixed in space with a frictional force that rotates around the disc was modelled. The expression obtained in the process of eliminating secular terms yields an unstable solution for modes with nodal diameters for arbitrary small friction forces. The backward travelling wave is destabilized by the friction. The angular speed of the travelling waves is ω_{rs}/s, where r is the number is the number of circumferential nodal lines, and s is the number of nodal diameters.

In a review on instabilities in discs given by Mottershead [26], a reference is made to an article by Chen and Bogy [27], where the forward wave is found to be destabilized by friction. When the review article refers to the work together with Motterhead and Chan [28], the statement on the direction of the wave is "The flutter instability was shown to result in waves that traveled forward and backward." Different articles and authors state the wave direction differently, and a clarification of this point may help to establish which mechanism may be responsible for squeal generation in a given situation.

The effect of follower forces, together with the effect of a negative friction velocity relationship, is investigated by Ouyang *et al.* [29]. The static disc is loaded by a rotating mass supported by two spring–damper systems in transverse and in-plane direction. A multiple scales analysis revealed the effect of negative friction velocity relationship as having a stabilizing influence on existing instabilities, while at the same time creating new instabilities. These new instabilities are seen to be destabilized by a transverse damper.

Tseng and Wickert [30] investigated a disc modelled as a thin annular plate subjected to a sector shaped follower force-type friction load. The model predicted critical modes at specified friction levels and varying angles of friction loading.

1.1.5. *Lining-deformation-induced instability*

The theories developed by Hultén [31] in the context of drum brake squeal are termed "lining-deformation-induced instability", and are basically an extension and refinement of the binary flutter mechanism. The basic achievement is the detailed explanation of the four mechanisms that in a drum brake leads to generation of travelling waves. These travelling waves occur as the sine and the cosine modes of the drum interact and couple at the same frequency. Models based on this mechanism have been able to simulate both frequencies and mode shapes of a squealing drum brake comparable to the measured results [32]. In the context of disc brake systems, waves travelling in the direction of rotation of the disc have been measured by Fieldhouse and Newcomb [33].

1.1.6. *Summary and discussion*

The mechanisms described above are listed here, with some remarks to indicate the field of research of the present work:

- *Stick-slip* does not produce a wave and cannot account for squeal, as the threshold of relative velocity is below what is relevant.
- *Negative μ-velocity slope* might contribute to instability, but does not in itself produce a wave in the disc. The effect of this mechanism is not considered here.
- *Sprag-slip or kinematic constraint* models are very simplistic and by themselves they are not well suited to model a complex disc brake.
- *Binary flutter* is a term for the state of oscillation, where energy is exchanged between two modes of vibration in a way that feed additional energy into the system. This is a wave-type motion and the effect is included in this model.
- *Follower forces* is a mechanism that can lead to binary flutter and produce travelling waves and the effect of this will be investigated here.
- *Lining deformation* can result in binary flutter and produce travelling waves and this mechanism is the main focus of this work.

The present work is an extension of the modelling work by North and an application of the lining deformation mechanism in the context of a disc brake system.

1.2. PRESENT WORK

In the present work, a simplified linear mathematical model of a disc brake is investigated, for the possible occurrence of unstable states of oscillatory motion. The investigation is done by performing an eigenvalue analysis of the characteristic matrix of the model of the system. A positive real part of a complex eigenvalue is seen as an indication of an instability, as it corresponds to an unbounded exponentially increasing amplitude of vibration. In a real brake system, such an initial instability is assumed to manifest itself as squeal, as it will grow to some level, where non-linear effects in the system will limit the amplitude to some state of stable oscillation. The study of these non-linear effects is beyond the scope of this paper.

The main objectives of the present work are to

- implement the disc and the pads as flexible components in the model of the disc brake system,
- incorporate the caliper as a rigid but not weightless member,
- as well as to judge the relative importance of the mechanisms proposed.

This work is concentrated on investigating the tendency of small vibrations to grow. For small vibrations, the temperature, speed and pressure are almost constant, and therefore a Coulomb friction model is sufficient.

The disc is modelled as a flexible beam with cyclo-symmetric boundary conditions and with a number of modes of vibration, sine and cosine modes. The model by North [18] had the limitation that the wavelength of the disc had to be nearly an order of magnitude larger than the length of the pad. This limitation can be relaxed by this modelling approach. It implies that the model has the ability to simulate squeal in a higher range of frequencies.

While the work of Mottershead focuses on the coupling by the follower force type of loading of the disc also inherent in the model of North, this work will focus on the moment created by the unequal size of the friction forces on each side of the disc by the difference in compression of the two friction materials. This moment tends to rotate the disc, as the transverse vibration occur, and this can generate a travelling wave.

Section 2 of the paper describes the system and the outline of the mathematical distributed-parameter model developed here. In section 2.1, the differential equation is derived for a friction loaded beam used for simulating the disc, while section 2.2 describes the more elaborate model and the method of discretization. Section 3 presents the results of the analysis and good correlation is found between frequencies of squeal measured in a vehicle and the response calculated with this model. Section 4 is the conclusion. Appendix A lists the equations for the extended model and Appendix B lists the parameters used in the model.

2. SYSTEM DESCRIPTION AND MATHEMATICAL MODEL

This work is based on a one-dimensional modelling approach. The basic equation for a flexible beam in contact with an elastic foundation is used to model the disc. An extended model is used when the discretization procedure is described and the results are generated.

2.1. A SIMPLE DISC INSTABILITY MODEL

The disc is modelled as a beam with an equivalent length L and is in sliding contact with an elastic medium (the friction material) over some length l, see Figure 1. The boundaries are constrained to secure cyclo-symmetric conditions and the shear deformation, rotary inertia and mounting of the disc are neglected. The disc and the friction materials are assumed to be in full contact. A constant Coulumb friction law is applied. Only transverse displacements are considered, but the contribution of the friction forces to the transverse force equilibrium and the moment equilibrium is included.

The most important factor in this modelling approach is the external bending moment on the disc. This moment is due to uneven friction forces of the two disc surfaces. An elastic deformation of the adjacent components produces an increase, respectively, a decrease, of the dynamic normal load. The moment stems from the two frictional forces each acting at a distance $h/2$ from the center of the disc, and each being different in size proportional to the displacement w, the stiffness of the lining material k_l and the friction μ. A follower force is generated due to the finite rotation of the disc element, see Figure 2. The differential equation for transverse vibration of the beam element representing the disc is

$$EI\frac{\partial^4 w}{\partial x^4} + \mu\frac{\partial w}{\partial x}k_l h + 2\mu N_0\frac{\partial w}{\partial x} + 2k_l w + m\frac{\partial^2 w}{\partial t^2} = 0. \tag{3}$$

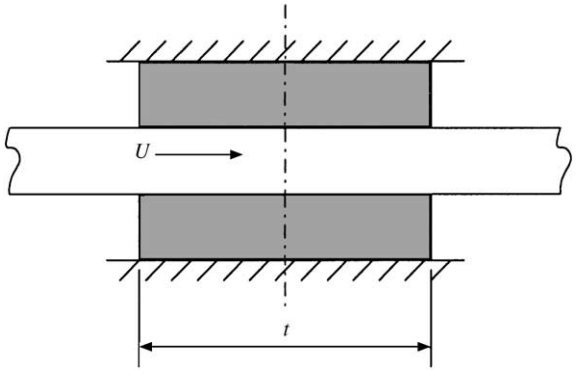

Figure 1. A beam model of the disc in contact with lining material acting as an elastic foundation.

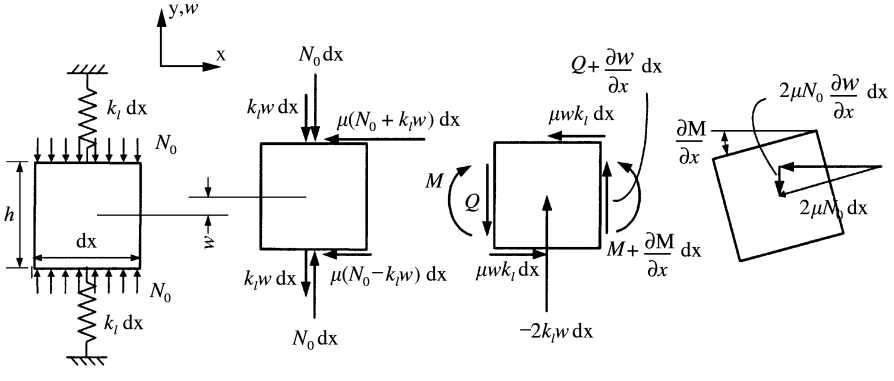

Figure 2. A segment of the disc in elastic contact with lining material. A normal preload pressure, N_0, is applied and the lining stiffness per length, k_l, creates a reaction force to the transverse displacement w. A moment $\mu k_l h w$ and a follower force $2\mu N_0 \partial w/\partial x$ are created due to translation and rotation respectively.

From equation (3) it can be readily seen that the two terms, $2\mu N_0 \partial w/\partial x$ and $\mu k_l h \partial w/\partial x$, both couple lateral displacement and rotation. The follower forces terms $2\mu N_0 \partial w/\partial x$ creates a transverse force given some rotation $\partial w/\partial x$, while the elastic deformation term $\mu k_l h \partial w/\partial x$ will create some bending moment, given some displacement w. These coupling terms can results in an unstable state of binary flutter, provided that some translational and rotational modes with eigenfrequencies in near proximity, are present in the coupled system.

The partial differential equation of motion for the simple system (3), can be transformed into a set of algebraic equations, by the use of the Galerkin method. The discrete equations of motion are then solved in terms of eigenvalues and eigenvectors.

As pointed out in the introduction, a perfect cyclo-symmetric structure, as an annular disc, has two modes of vibration with the same natural frequency. When some external disturbance (contact with the friction material) is applied, the frequency of these modes will change, and they will separate, so they no longer have the same frequency. The action of the coupling terms discussed here, is to make these modes appear at the same freqeuncy and interact in an unstable manner. The aim of the model is to judge the relative importance of the two coupling terms. The dissipative effects in the real brake system are

not included in this model, as they are assumed not to change the fundamental behaviour of the system.

In this simple example, the equation of the motion for a system with both follower forces and lining deformation induced instability is discussed. Next, an extended model will be used, in order to achieve results in terms of frequencies and mode shapes.

2.2. EXTENDED MODEL

The model presented here consists of both rigid and flexible parts. This disc is modelled as a continuous member, in the form of a one-dimensional beam with cyclo-symmetric boundary conditions. The disc can be viewed as a two-dimensional annular plate, and by reducing it to a one-dimensional structure, the variations in stress, strain and deflection over the width can be ignored. This means that mode shapes involving nodal circumferential lines cannot be represented by the model and it effectively limits the scope of the analysis to solutions involving ω_{0s}, where s is the number of nodal diameters. Measurements on squealing disc brakes show this to be the usual modeshape [33, 34], and to keep things simple and still sufficiently accurate, the one-dimensional representation has been chosen. The pads are also represented by continuous elements as beams.

Figure 3 shows a model of the brake system to be analyzed, where the disc (1) and the two pads, (2) and (3), are connected by the friction material, which is modelled as an infinite number of springs. The backplates of the pads are the main contributers to their stiffness, so they are represented by beams, while the friction material is represented by springs that are able to account for the variation in distance between backplate and disc. The derivation of equation (3) is based on a beam on an elastic foundation. In the present model, the disc is a beam in elastic contact with other beams that represent the backplate of the pads. At the abutment, the backplates are in contact with a part of the brake, which is not included in this model, and thus only represented by a flexible contact with ground.

The pistons, (4) and (5), are modelled as rigid bodies, with 1 d.o.f. in the lateral direction. They are in contact with the backplate of the inboard pad by means of seven springs representing the distributed contact. As the pistons are rigid bodies their connection to the caliper can be represented by single springs.

The caliper consists of two parts, (6) and (7), each with 2 d.o.f., one translation in the lateral direction and one rotation about the center of gravity. The caliper is connected to ground via two springs, located at the point of contact between caliper pins and the brake carrier.

The general formulation of an equation of motion for a continuous, linear system without external excitation can be given in the following form:

$$M[\ddot{w}] + L[w] = 0, \tag{4}$$

where L and M are linear differential operators. The partial differential equation (4) can be discretized to a system of ordinary equations by employing the Galerkin method. In a matrix formulation, the stiffness and mass terms are generated as follows:

$$k_{ij} = \int_D \phi_i L[\phi_j]\,\mathrm{d}D \quad \text{and} \quad m_{ij} = \int_D \phi_i M[\phi_j]\,\mathrm{d}D, \tag{5,6}$$

where D is the domain of integration, i.e., the length of the continuous component, ϕ are testfunctions, $i,j = 1, 2 \ldots, N$, and N is the number of terms included in the analysis [35].

The quality of this discretization depends heavily on the choice and the number of test functions. If ϕ_i are the eigenfunctions for the eigenvalue problem $L[\phi] = \lambda M[\phi]$ corresponding to equation (4), then the results of the discretized system of equations

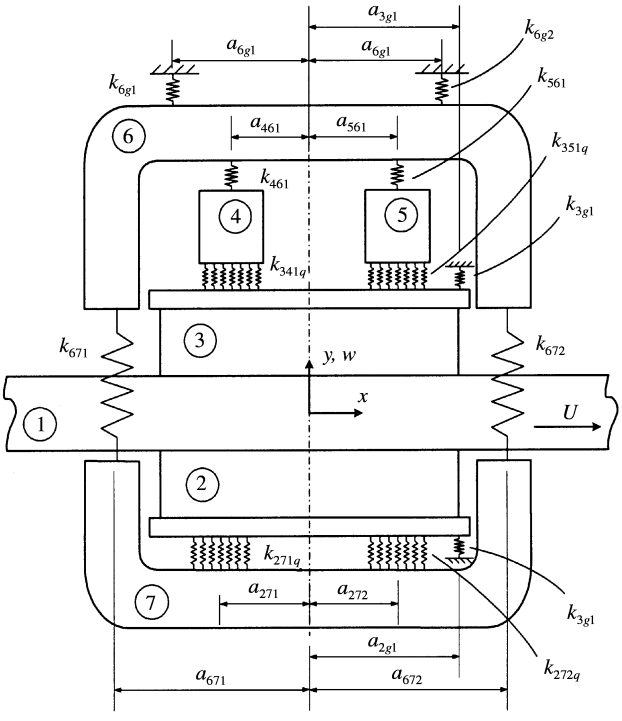

Figure 3. A disc brake model with disc (1) and pads (2) and (3) as continuous elements. Pistons (4) and (5) and the caliper parts (6) and (7) are discrete elements.

are identical to the results from the original differential equation. By selecting the eigenfunctions of the associated free–free parts as the test functions, for moderate system coupling the result will be close to the true value, even for a reasonable low number of test functions. As these eigenmodes constitute a complete infinite orthogonal set, the solutions will converge to the correct solution, as the number of functions included is increased towards infinity.

For the disc, the testfunctions chosen for calculating the matrix elements according to equations (5) and (6), are the eigenfunctions of a beam with cyclo-symmetric boundary conditions [36], i.e., the sine and cosine functions as defined by

$$\phi_1(n,x) = \begin{cases} \sin\left(\dfrac{2\pi x}{L}\dfrac{n+1}{2}\right) & \text{for odd } n, \\ \cos\left(\dfrac{2\pi x}{L}\dfrac{n}{2}\right) & \text{for even } n, \end{cases} \quad -\frac{L}{2} < x < \frac{L}{2}, \tag{7}$$

where the subscript 1 indicates the disc and the argument n indicates the mode number. The pads are assumed to have two rigid-body modes (lateral translation and rotation) and a set of flexible modes

$$\phi_p(n,x) = \begin{cases} 1 & \text{for } n = 1 \\ \dfrac{2x}{l} & \text{for } n = 2 \quad \text{for } p = 2,3 \quad \text{and} \quad -\frac{1}{2} < x < \frac{1}{2}, \\ y_n(x) & \text{for } n > 2 \end{cases} \tag{8}$$

where $y_n(x)$ are eigenfunctions for a free–free Euler–Bernoulli beam

$$y_n(x) = a_n \sin \beta_n x + b_n \cos \beta_n x + c_n \sinh \beta_n x + d_n \cosh \beta_n x. \tag{9}$$

The pistons have only 1 d.o.f.: Rigid body lateral displacement

$$\phi_p(1) = 1 \quad \text{for } p = 4, 5. \tag{10}$$

The two caliper parts have two rigid-body modes, one for translation and another for rotation:

$$\phi_p(n, x) = \begin{cases} 1 & \text{for } n = 1 \\ \dfrac{2x}{L_p} & \text{for } n = 2 \end{cases} \quad \text{for } p = 6, 7 \text{ and } -\frac{L_p}{2} < x < \frac{L_p}{2}. \tag{11}$$

Appendix A lists the partial differential equations for the extended system, together with the integral functions used for calculation of the stiffness terms. The complex eigenvalues are calculated and a positive real and imaginary part corresponds to an exponentially increasing oscillatory amplitude of vibration.

2.3. ESTIMATING PARAMETERS FOR THE MODEL

The parameters used in the modelling of the main components, disc and pads, have been established by a least-squares estimation, based on the measured modal properties of the disc brake hardware. The parameters used in the calculations are listed in Appendix B. The brake is an air activated disc brake for heavy vehicles. The disc is an annular plate connected to the hub via a spline. Bae and Wicker [37] have reported that modes with almost identical out-of-plane vibration patterns can exist in sets of two. Modes without circumferential nodal lines can be represented both as conventional out-of-plane bending modes or as in-plane modes that couple to out-of-plane modes via the hat section. These second modes are not present in this case, as no hat section is there to act as a coupling agent.

The frequencies measured on the disc for modes with nodal diameters are shown in Table 1. Measured frequencies are obtained by experimental modal analysis performed on the mounted disc using the impact excitation method. The calculated resonance frequencies are based on the Euler–Bernoulli beam theory. The disc modes with nodal circumferential lines are not included in this analysis. The out-of-plane vibration of the disc on a circumferential line, can be described by the same functions as the eigenfunctions of a cyclo-symmetric beam (sine or cosine functions). At the same time, the measured and calculated frequencies are in fairly good agreement, except for the lowest mode.

In a similar way, the parameters for the pads are estimated based on the measured data indicated in Table 2. The pads are measured in a free–free condition. They have an irregular shape and only three of the lowest measured modes can easily be identified as

TABLE 1

Comparison of measured and calculated modal properties of the disc

Number of nodal diameters	2	3	4	5	6	7	8	
Measured frequency	755	1893	3332	4962	6710	8531	10398	Hz
Calculated frequency	1272	1887	2964	4450	6312	8535	11111	Hz
Difference	68·5	−0·3	−11·0	−10·3	−5·9	0·0	6·8	%

TABLE 2

Comparison of experimental results and calculated frequencies for the pads

Number of nodal lines	2	3	4	
Measured frequency	752	1828	3521	Hz
Calculated frequency	697	1922	3768	Hz
Difference	−7·3	5·2	7·0	%

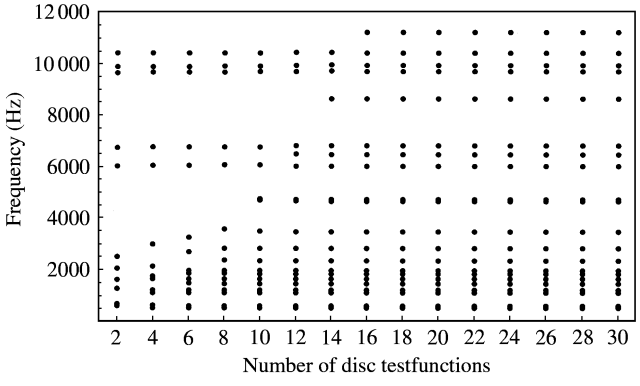

Figure 4. Convergence of the response for addition of testfunctions for the disc. Twenty pad testfunctions are included in this calculation. Disc testfunctions are added in pairs of doublet disc modes. The number of nodal diameters are equal to half the number of disc testfunctions.

bending modes. Higher modes include some amount of torsion and the higher pad testfunctions included in the calculations are the higher order beam bending modes calculated from the parameters obtained from the lowest modes. The bending stiffness of the pads EI_p, $p = 2, 3$, account for the bending stiffness of the steel backplate and the friction material.

2.4. CHECK FOR CONVERGENCE OF THE SOLUTION

To choose the appropriate number of testfuctions, it is necessary to check the convergence of the solution. In the coupled system, the properties of the disc and the pads have to be represented by enough testfunctions, to give a converged solution within the frequency range of interest.

In a series of calculations, the number of disc testfunctions where increased from 2 to 30. In the results of the calculations, the lowest eigenvalues quickly converge, while the high-frequency response of the system is dependent on the higher order testfunctions and hence more functions are needed. The convergence of the eigenvalues is shown in Figure 4. With 14 testfunctions or less a mode of vibration at 11.3 kHz cannot be represented, while the inclusion of 30 testfunctions instead of 20 only changes the high-frequency response by 0.04%. The figure shows the imaginary part of the eigenvalue (the frequency), and a study of the real part of the eigenvalue (not displayed) converged in the same manner.

In a subsequent series of calculation, the number of pad testfunctions was increased from 3 to 30, and the result is as indicated in Figure 5. A mode near 11.3 kHz is present already after the first two testfuctions (translation and rotation of the pads). The error decreases monotonically from 14 testfunctions and the difference by using 30 testfunctions

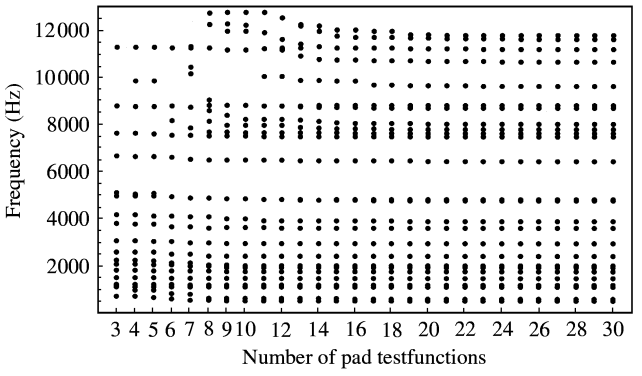

Figure 5. Convergence of response for addition of pad testfunctions. Twenty testfunctions are included are included in this analysis. The frequency close to 11·3 kHz change $<0{\cdot}2\%$ from 20 to 30 pad testfuctions.

instead of 20 is $<0{\cdot}2\%$. The main reason for the slow convergence of this mode is the fact that contact between backplate and piston/caliper is modelled as a zone of contact (the seven springs). This gives rise to edge effects and a relative high number of modes are needed to accommodate for the abrupt change in contact configuration. If the springs $k_{271q}, k_{272q}, k_{341q}$ and k_{351q} are made softer, the convergence is much quicker.

Based on these results, the system has been laid out include 20 disc testfunctions and 20 pad testfuctions, and together with the pistons and caliper this adds up to a total of 66 d.o.f.

In this section the differential equations for a friction loaded beam representing a disc are derived and the discretization of a distributed-parameter simple model of a disc brake is developed. The type and the number of testfunctions needed to calculate the response is chosen, and the next section will present some results obtained from calculations using this model.

3. RESULTS

The system has two eigenvalues with positive real part within the frequency range of interest. In Table 3, calculated and measured frequencies are shown. The squeal frequencies in the first row of the table are measured on a vehicle equipped with the brake system analyzed. In the second row, the unstable frequencies of the model are shown. The result indicated as (8780) emerges at a higher level of friction ($\mu \approx 0{\cdot}5$) compared to the baseline friction on 0·35). Friction levels are known to vary (with temperature, etc.), but the extent of this variation in the present case and whether it corresponds to the situation generating squeal at 8·6 kHz is not known. Experimenting with parameter changes has shown that the model can predict some low-frequency squeal that is not measured during testing. The differences in the numbers between the comparable frequencies in Table 3 are small. The measured squeal is the stable oscillatory limit-cycle response of a real, non-linear and damped system. The calculated frequencies indicate the onset of small vibrations in a linear model, and as both damping and non-linear effects will influence the frequency, differences are to be expected. However, differences with a similar tendency are seen in comparing eigenfrequencies measured on the disc and frequencies calculated using the Euler–Bernoulli beam theory, see Table 1, so maybe a better representation of the disc in the model could reduce the differences.

TABLE 3

Comparison of measured squeal and frequencies calculated in the current model

Squeal measured in vehicle [38]	6850	8600	10 550	Hz
Calculated frequencies	6452	(8780)	11 243	Hz
Difference	−5·8	(2·1)	6·6	%
Calculated number of nodal diameters	6	7	8	

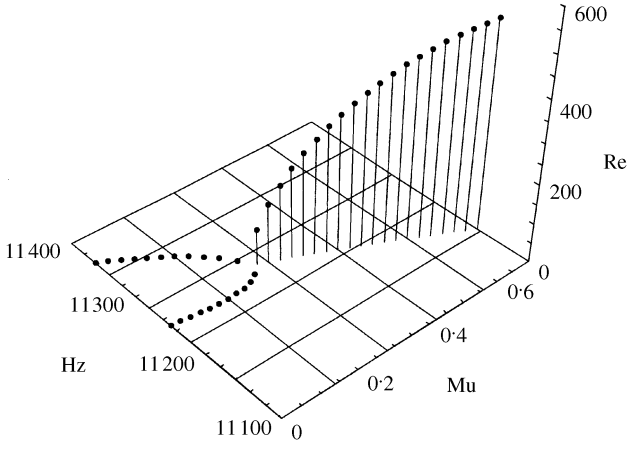

Figure 6. A trace of eigenvalues near 11 300 Hz for a variation of μ from 0 to 0·7. Two modes couple at the same frequency and the real part increases.

The reason for the good agreement between measured squeal and calculated instability is probably due to the fact that these particular squeals are close to disc resonance frequencies. Furthermore, some of the parameters of the model are estimated. Experimenting with changes within reasonable limits has shown that these parameters may influence the instability level, but they have only a limited effect on the estimated instability frequencies. The measured squeal in this case is close to the disc eigenfrequencies and this model is able to represent the disc response fairly well. The good agreement between the measured squeal and the calculated instability may be due to the squeal being generated by a coupling of disc modes, and this coupling may be due to a mechanism as the one described here.

3.1. DECOUPLING AND COUPLING OF MODES

The perfect cyclo-symmetric annular disc has two modes of vibration with the same frequency. The location of the nodal diameters is not fixed, until some external disturbance interacts with the structure. The localization of the modes and the violation of the cyclo-symmetric configuration lead to a split of the frequencies of the two modes. At the same time, other modes of the system are changed due to the stress stiffening or mass loading effect of the coupling interaction.

The eigenvalues of the system are calculated for an increase in friction level μ from 0 to 0·7. In Figure 6, the coupling of the modes near 11 300 Hz are shown. For a value of μ around 0·2 the two modes merge at the same frequency and the real part of the eigenvalue

moves in the positive direction, as an indication of the destabilizing effects exerted by the friction forces.

3.2. MODES OF VIBRATION

The deflection shapes can be plotted based on the eigenvector associated with a given eigenvalue. The shapes corresponding to one of the unstable modes are plotted in Figure 7. The thick solid line in the middle is the disc and the two thin adjacent lines are the pads. The two thick straight lines above and below are the caliper halves and the two short lines are the pistons.

This mode shows a disc wave (with six nodal diameters) travelling in the direction of rotation of the disc. The present model can predict such a travelling wave, as the existence of "sine" and "cosine" testfunctions with complex amplitudes can combine to form a travelling wave if an eigenvector with appropriate amplitude and phase is calculated.

A travelling wave is a complex mode of vibration, as opposed to a normal mode or a synchronous mode. A synchronous mode can be represented by a real eigenvector and it will be stable, as a real eigenvector is associated with a real eigenvalue. In the context of a real undamped system, the opposite statement is true: A non-synchronous mode or its complex conjugate neighbor is unstable, as at least one of these eigenvalues will have a positive real part.

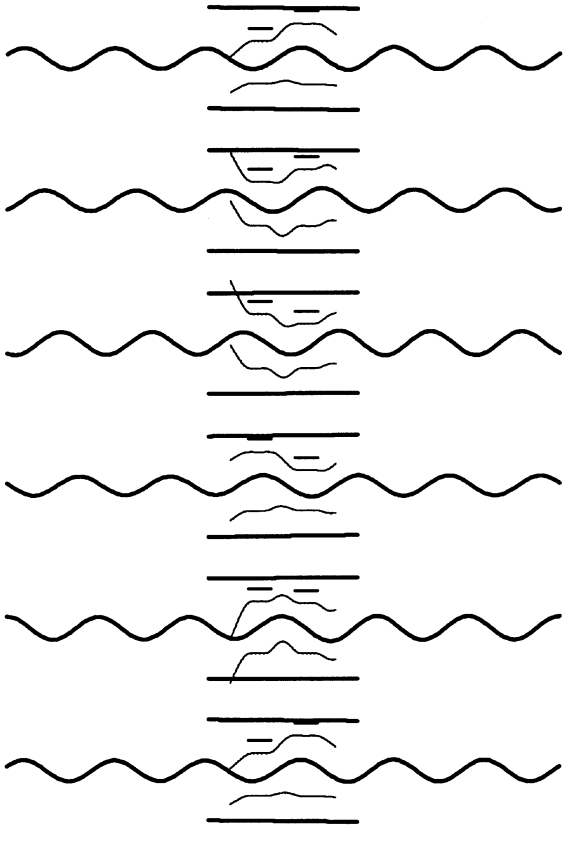

Figure 7. Mode at 6452 Hz. Six instantaneous deflection shapes of the system during a 0–2π vibration cycle. By following a point of maximum amplitude on the disc, the wave can be seen to travel in the direction of rotation of the disc (to the right).

The modes of vibration in this disc brake system has not yet been measured during operating conditions, but the measurements of Fieldhouse and Newcomb on a disc brake system [33], show a similar forward travelling wave pattern. In a drum brake system, Hultén *et al*. [32] have measured a travelling wave in the direction of drum rotation, during a stop with squeal.

3.3. THE EFFECT OF FOLLOWER FORCES

The relative effect of follower forces and of the moment generated by variation in friction forces are considered.

The instability in the mathematical model arises from the non-symmetry in the stiffness matrix. A real symmetric matrix will always be associated with real eigenvalues and hence a system with stable solutions. The terms responsible for non-symmetry in the simple formulation described by equation (3) is related to follower forces $2\mu N_0 \partial w/\partial x$ and to lining deformation induced couplings $\mu k_l h \partial w/\partial x$. These terms enter the equations at the same location, but their numerical value is very different for the configuration considered here. The ratio between the follower forces and the lining deformation coupling is

$$\frac{2\mu N_0 \partial w/\partial x}{\mu k_l h \partial w/\partial x} = \frac{2N_0}{k_l h}. \tag{12}$$

For the normal force, $N_0 = 1 \times 10^5$ N/m, corresponding to a brake application with a deceleration of $1{\cdot}6\,\mathrm{m/s^2}$, a lining stiffness $k_l = 1{\cdot}215 \times 10^{10}$ N/m/m and a disc thickness $h = 0{\cdot}045$ m, the result is a ratio of $3{\cdot}66 \times 10^{-4}$ and even for a very thin disc of $h = 0{\cdot}001$ m, the ratio is as low as $1{\cdot}65 \times 10^{-2}$.

In the extended model, the configuration is more complicated as the ratio involves the displacement of the disc as well as the pads, i.e.,

$$\frac{2\mu N_0 \partial w_1/\partial x}{\mu k_l (h/2)(2\partial w_1/\partial x - \partial w_2/\partial x - \partial w_3/\partial x)}. \tag{13}$$

The stiffness matrix can be separated into terms

$$[\mathbf{K}] = [\mathbf{K}]|_{\mu=0} + [\mathbf{K}]_{FF} + [\mathbf{K}]_{LD}, \tag{14}$$

where $[\mathbf{K}]|_{\mu=0}$ is the symmetric matrix for $\mu = 0$, $[\mathbf{K}]_{FF}$ is the non-symmetric matrix of terms generated by follower forces and $[\mathbf{K}]_{LD}$ is the non-symmetric matrix of terms generated by lining deformation. On average, the non-zero terms of $[\mathbf{K}]_{FF}$ are 0.45% of the corresponding terms in $[\mathbf{K}]_{LD}$. The largest relative term is 6·1% but this term in $[\mathbf{K}]_{FF}$ is only $1{\cdot}01 \times 10^{-5}$% of the largest terms in $[\mathbf{K}]_{LD}$. The ratio of the norms is

$$\frac{\|[\mathbf{K}]_{FF}\|}{\|[\mathbf{K}]_{LD}\|} = 1{\cdot}18625 \times 10^{-4}, \tag{15}$$

where $\|\mathbf{C}\| = \sqrt{\Sigma_i \Sigma_j c_{ij}^2}$ is the Frobenius norm of some matrix $\mathbf{C}$.

These numerical comparisons indicate that the follower force contribution to the instability in a model like this is negligible.

4. CONCLUSION

In this paper, a series of mechanisms for disc brake squeal are considered. Negative μ-velocity slope as well as stick–slip is discussed and proved not to be important by other authors. The effect of follower forces as well as lining-deformation-induced couplings are investigated. The effect of follower forces is shown to be marginal. On the other hand,

according to this model, the lining-deformation-induced couplings can be of significant importance, as a factor in generating instabilities.

The modelling approach using a continuous model in combination with the Galerkin method is shown to be an effective way of modelling the complexity of the modes of vibration with only a limited number of degrees of freedom. The convergence of the solution is rapid. Only 66 testfunctions are needed. A further advantage with the modelling technique is that the parameters (like for instance the bending stiffness $EI(x)$) might have any function representation. Therefore, such a model is very well suited for sensitivity analysis.

The results show good agreement with squeal measured in a vehicle test with a brake system as the one modelled here. The disc in this case seems to be a dominating factor in deciding the squeal frequencies and the model can simulate the disc vibration fairly closely. The modes of vibration calculated for this configuration has the distinct feature of a forward travelling wave. The verification of this mode of vibration has not yet been made on this specific brake system, but the measurements on a similar brake type has shown a forward travelling wave pattern.

The detailed study of the effects of decoupling and coupling of modes allows for a better understanding of the mechanisms leading to instability, and it allows for investigations of changes leading to favorable system configurations.

ACKNOWLEDGMENTS

We wish to thank the referees for the thorough reading and for the suggestions of enhancements and changes to this paper. We would also like to thank Meneta Advanced Shims Technology A/S and Volvo Truck Corporation for permission to publish this work.

REFERENCES

1. R. A. Ibrahim 1992 *Friction-Induced Vibration, Chatter, Squeal, and Chaos* (R. Ibrahim and A. Soom, editors), DE-Vol. 49, 107–121. New York: American Society of Mechanical Engineers. Friction-induced vibration, chatter, squeal, and chaos. Part 1 mechanics of friction.
2. R. A. Ibrahim 1992 *Friction-Induced Vibration, Chatter, Squeal, and Chaos* (R. Ibrahim and A. Soom, editors), DE-Vol. 49, 123–138. New York: American Society of Mechanical Engineers. Friction-induced vibration, chatter, squeal, and chaos. Part 2 dynamics and modeling.
3. P. Basford and S. Twiss 1958. *Transactions of the American Society of Mechanical Engineers* **80**, 402–406. Properties of friction materials. I—experiments on variables affecting noise.
4. P. Basford and S. Twiss 1958. *Transactions of the American Society of Mechanical Engineers* **80**, 407–410. Properties of friction materials. II—theory of vibration in brakes.
5. A. Banerjee 1968 Wear **12**, 107–116. Influence of kinetic friction on the critical velocity of stick–slip motion.
6. E. Brommundt 1995 *Zeitschrift für angewandte Mathematik und Mechanik* **75**, 811–820. Ein Reibschwinger mit Selbsterregung ohne fallende Reibkennlinie.
7. J. H. Smith and J. Woodhouse 2000 *Journal of the Mechanics and Physics of Solids* **48**, 1633–1681. The tribology of rosin.
8. R. Spurr 1961–62 *Proceedings of the Institution of Mechanical Engineers* **1**, 33–40. A theory of brake squeal.
9. R. Spurr 1971 *Proceedings of the Institution of Mechanical Engineers* **C95/71**, 13–16. Brake squeal.
10. R. Jarvis and B. Mills 1963–64 *Proceedings of the Institution of Mechanical Engineers* **178**, 847–866. Vibrations induced by dry friction.

11. S. Earles and G. Soar 1971 *Proceedings of the Institution of Mechanical Engineers* **C101**, 61–69. Squeal noise in disc brakes.
12. S. Earles and G. Soar 1974 *Institute of Physics, Stress Analysis Group, Annual Conference* 237–251. A vibrational analysis of a pindisc system with particular reference to squeal noise in disc-brakes.
13. S. Earles and M. Badi 1978 *Society of Automotive Engineers* SAE780331 1–8. On the interaction of a two-pin-disc system with reference to the generation of disc-brake squeal.
14. H. Busby, W. Lyons and R. Singh 1985 *Noise-Con* 85, *The Ohio State University* 227–234. Stability analysis of a brake squeal model.
15. N. Millner 1978 *Society of Automotive Engineers* SAE780332. An analysis of disc brake squeal.
16. H. Murakami, N. Tsunada and T. Kitamura 1984 *Society of Automotive Engineers* SAE841233. A study concerned with a mechanism of disc brake squeal.
17. M. Nishiwaki 1993 *Proceedings of the Institution of Mechanical Engineers* **207**, 195–202. Generalized theory of brake noise.
18. M. North 1972 *Ph.D. Thesis, Loughborough University of Technology*. Frictionally induced, selfexcited vibrations in a disc brake system.
19. M. North 1972 *Technical Report* 1972/5, The motor industry research association. Disc brake squeal—a theoretical model.
20. M. North 1976 *Proceedings of the Institution of Mechanical Engineers* **C38/76**, 169–176. Disc brake squeal.
21. P. Brooks, D. Crolla and A. Lang 1992 *AVEC* **1992.9**, 28–36. Sensitivity analysis of disc brake squeal.
22. P. C. Brooks, D. Crolla, A. M. Lang and D. Schafer 1993 *Proceedings of the Institution of Mechanical Engineers* **C444/004**, 135–143. Eigenvalue sensitivity analysis applied to disc brake squeal.
23. Y. Yuan 1995 in *1995 American Society of Mechanical Engineers. Design Engineering Technical Conferences*, Vol. 3, DE-Vol. 84-1, 1153–1162. A study of the effects of negative friction-speed slope on brake squeal.
24. J. Mottershead and S. Chan 1992 in *Friction-Induced Vibration, Chatter, Squeal, and Chaos* (R. Ibrahim and A. Soom, editors), DE-Vol. 49, 87–97. New York: American Society of Mechanical Engineers. Brake squeal—an analysis of symmetry and flutter instability.
25. S. Chan, J. Mottershead and M. Cartmell 1995 *Transactions of the American Society of Mechanical Engineers, Journal of Vibration, And Acoustics* **117**, 240–242. Instabilities at subcritical speeds in disc with rotating frictional follower loads.
26. J. Mottershead 1998 *The Shock and Vibration Digest* **30**, 14–31. Vibration- and friction-induced instabilities in disks.
27. J. Chen and D. Bogy 1992 *Transactions of the American Society of Mechanical Engineers, Journal of Applied Mechanics* **59**, 5230–5235. Effects of load parameters on the natural frequencies and stability on a flexible spinning disk with a stationary load system.
28. J. Motterhead and S. Chan 1995 *Transactions of the American Society of Mechanical Engineers, Journal of Vibration and Acoustics* **117**, 161–163. Flutter instability of circular discs with frictional follower loads.
29. H. Ouyang, J. Mottershead, M. Cartmell and M. Friswell 1998 *Journal of Sound and Vibration* **209**, 251–264. Friction-induced parametric resonances in discs: effect of a negative friction-velocity relationship. doi:10.1006/jsvi.1997.1261.
30. J-G. Tseng, J. A. Wickert 1998 *Transactions of the American Society of Mechanical Engineers, Journal of Vibration and Acoustics* **120**, 922–929. Nonconservative stability of a friction loaded disk.
31. J. Hultén 1995 *Proceedings of the* 1995 *Noise and vibration Conference, Vol 1* (*Traverse City, Michigan*), *SAE Paper* 951280, 377–388. Some drum brake squeal mechanisms.
32. J. Hultén, J. Flint and T. Nellemose 1997 *Society of Automotive Engineers* SAE972028. Mode shape of a squealing drum brake.
33. J. Fieldhouse and T. Newcomb 1996 *Optics and Lasers in Engineering* **25**, 455–494. Double pulsed holography used to investigate noisy brakes.
34. A. Felske and A. Happe 1977 *Automobiltechnische Zeitschrift* **79**, 281–288. Quietschen von Schiebenbremsen—Holographische Schwingungsanalyse und Abhilfemassnahmen.
35. L. Meirovitch 1967 *Analytical Methods in Vibrations*. New York: The MacMillan Company.
36. J. Hultén and J. Flint 1999 *Society of Automotive Engineers* SAE1999-01-1335. An assumed modes method approach to disc brake squeal analysis.

37. J. BAE and J. WICKERT 2000 *Journal of Sound and Vibration* **235**, 117–132. Free vibration of coupled disk-hat structures. doi:10.1006/jsvi.2000.2914.
38. J. HULTÉN 2000 *Technical Report* 20000714, Internal Report. Volvo Truck Corporation.

APPENDIX A. SYSTEM EQUATIONS

The differential equations for the three continuous elements of the extended system are

$$EI_1\frac{\partial^4 w_1}{\partial x^4} + \mu k_l \frac{h}{2}\left(2\frac{\partial w_1}{\partial x} - \frac{\partial w_2}{\partial x} - \frac{\partial w_3}{\partial x}\right) + k_l(2w_1 - w_2 - w_3) + k_m w_1 + 2\mu N_0 \frac{\partial w_1}{\partial x} + m_1 \frac{\partial^2 w_1}{\partial t^2} = 0, \tag{A.1}$$

$$EI_2 \frac{\partial^4 w_2}{\partial x^4} + \mu k_l\, t\left(\frac{\partial w_1}{\partial x} - \frac{\partial w_2}{\partial x}\right) - k_l(w_1 - w_2) - \mu N_0 \frac{\partial w_1}{\partial x} + \sum_{p=1}^{2}\sum_{q=1}^{7} k_{27pq}\delta(x - a_{27pq})(w_7 - w_2) + k_{2g1}\delta(x - a_{2g1})w_2 + m_2 \frac{\partial^2 w_2}{\partial t^2} = 0, \tag{A.2}$$

$$EI_3\frac{\partial^4 w_3}{\partial x^4} + \mu k_l\, t\left(\frac{\partial w_1}{\partial x} - \frac{\partial w_3}{\partial x}\right) - k_l(w_1 - w_3) - \mu N_0\frac{\partial^2 w_2}{\partial t^2} + \sum_{p=4}^{5}\sum_{q=1}^{7} k_{3p1q}\delta(x - a_{3p1q})(w_p - w_3) + k_{3g1}\delta(x - a_{3g1})w_3 + m_3 \frac{\partial^2 w_3}{\partial t^2} = 0, \tag{A.3}$$

where index 1 is for the disc and 2,3 is for the pads. In the double summation in equation (A.2), the index p represents the two locations of contact between pad and caliper, and the index q represents the seven discrete springs that has been used to model the distributed contact at each location. In equation (A.3), the index p represents the spring endpoints on either of the two pistons.

Equations (A.1)–(A.3) can be expressed in terms of operators as follows:

$$L_i[w_1, w_2, w_3] + M_i[\ddot{w}_i] = 0, \tag{A.4}$$

where $i = 1, 2, 3$ and

$$L_1 = L_{L1} + L_{l1}, \tag{A.5}$$

$$L_{L1} = EI_1\frac{\partial^4 w_1}{\partial x^4} + k_m w_1, \tag{A.6}$$

$$L_{l1} = \mu k_1 \frac{h}{2}\left(2\frac{\partial w_1}{\partial x} - \frac{\partial w_2}{\partial x} - \frac{\partial w_3}{\partial x}\right) + k_1(2w_1 - w_2 - w_3) + 2\mu N_0\frac{\partial w_1}{\partial x}, \tag{A.7}$$

$$M_1 = m_1 w_1 \tag{A.8}$$

and for the two pads

$$L_2 = EI_2 \frac{\partial^4 w_2}{\partial x^4} = \mu k_l\, t\left(\frac{\partial w_1}{\partial x} - \frac{\partial w_2}{\partial x}\right) - k_l(w_1 - w_2) - \mu N_0\frac{\partial w_1}{\partial x} + \sum_{p=1}^{2}\sum_{q=1}^{7} k_{27pa}\delta(x - a_{27pq})(w_7 - w_2) + k_{2g1}\delta(x - a_{2g1})w_2, \tag{A.9}$$

$$L_3 = EI_3 \frac{\partial^4 w_3}{\partial x^4} + \mu k_l\, t\left(\frac{\partial w_1}{\partial x} - \frac{\partial w_3}{\partial x}\right) - k_l(w_1 - w_3) - \mu N_0 \frac{\partial w_1}{\partial x} + \sum_{p=4}^{5}\sum_{q=1}^{7} k_{3p1q}\delta(x - a_{3p1q})(w_p - w_3) + k_{3g1}\delta(x - a_{3g1})w_3, \tag{A.10}$$

and $M_i = m_i w_i$, where $i = 2, 3$. The elements of the stiffness matrix are calculated according to the equations below. For the disc, the following applies for calculating the terms:

$$k_{1,1}(i,j) = \int_{-l/2}^{l/2} \phi_1(i,x) L_{l1}[\phi_1(j,x), 0, 0]\,\mathrm{d}x + \int_{l/2}^{l/2} \phi_1(i,x) L_{L1}[\phi_1(j,x)]\,\mathrm{d}x, \tag{A.11}$$

$$k_{1,2}(i,j) = \int_{-l/2}^{l/2} \phi_1(i,x) L_{l1}[0, \phi_2(j,x), 0]\,\mathrm{d}x, \tag{A.12}$$

$$k_{1,3}(i,j) = \int_{-l/2}^{l/2} \phi_1(i,x) L_{l1}[0, 0, \phi_3(j,x)]\,\mathrm{d}x, \tag{A.13}$$

$$k_{1,p}(i,j) = 0 \quad \text{for } p = 4, 5, 6, 7, \tag{A.14}$$

where the notation $k_{1,p}(i, j)$ is adopted for the element of the submatrix ith, jth element of the submatrix 1, p that represents the elastic stiffness between the disc (body 1) and the body represented by p. The matrix elements of the submatrix representing body two:

$$k_{2,1}(i,j) = \int_{-l/2}^{l/2} \phi_2(i,x) L_2[\phi_1(j,x), 0, 0, 0]\,\mathrm{d}x, \tag{A.15}$$

$$k_{2,2}(i,j) = \int_{-1/2}^{1/2} \phi_2(i,x) L_2[0, \phi_2(j,x), 0]\,\mathrm{d}x, \tag{A.16}$$

$$k_{2,p}(i,j) = 0 \quad \text{for } p = 3, 4, 5, 6, \tag{A.17}$$

$$k_{2,7}(i,j) = \sum_{p=1}^{2}\sum_{q=1}^{7} [k_{27pq}\phi_2(i, a_{27pq})\phi_2(j, a_{27pq})]. \tag{A.18}$$

The matrix elements representing body three:

$$k_{3,1}(i,j) = \int_{-l/2}^{l/2} \phi_3(i,x) L_3[\phi_1(j,x), 0, 0]\,\mathrm{d}x, \quad k_{3,2}(i,j) = 0, \tag{A.19}$$

$$k_{3,3}(i,j) = \int_{-l/2}^{l/2} \phi_3(i,x) L_3[0, 0, \phi_3(j,x)]\,\mathrm{d}x, \tag{A.20}$$

$$k_{3,p}(i,j) = \begin{cases} -\sum_{q=1}^{7} k_{3p1q}\phi_3(i, a_{3p1q})\phi_3(j, a_{3p1q}) & \text{for } p = 4, 5, \\ 0 & \text{for } p = 6, 7. \end{cases} \tag{A.21}$$

For the pistons, $p = 4, 5$, the following stiffness terms are valid:

$$k_{p,1}(i,j) = 0,\ k_{p,2}(i,j) = 0,\ k_{p,3}(i,j) = k_{3p}\phi_3(i, a_{3p})\phi_3(j, a_{3p}), \tag{A.22}$$

$$k_{p,q}(i,j) = -\delta_{pq}\left(\sum_{r=1}^{7} k_{3p1r} + k_{6p}\right) \quad \text{for } q = 4, 5, \tag{A.23}$$

$$k_{p,6}(i,j) = k_{p6}\phi_6(i,a_{p6})\phi_6(j,a_{p6}), \quad k_{p,7}(i,j) = 0, \tag{A.24}$$

where δ_{pq} is Kroneckers delta

$$\delta_{pq} = \begin{cases} 1 & \text{if } p = q, \\ 0 & \text{if } p \neq q, \end{cases}$$

the caliper part (6) on the piston side has the following stiffness terms:

$$\begin{aligned} &k_{6,1}(i,j) = 0, \ k_{6,2}(i,j) = 0, \ k_{6,3}(i,j) = 0, \\ &k_{6,p}(i,j) = k_{p6} \quad \text{for } p = 4,5, \end{aligned} \tag{A.25}$$

$$k_{6,6}(i,j) = -\sum_{p=4}^{5} k_{p6}\phi_6(i,a_{p6})\phi_6(j,a_{p6}) - \sum_{p=1}^{2} k_{6gp}\phi_6(i,a_{6gp})\phi_6(j,a_{6gp}), \tag{A.26}$$

$$k_{6,7}(i,j) = \sum_{p=1}^{2} k_{67p}\phi_6(i,a_{67p})\phi_7(j,a_{67p}). \tag{A.27}$$

The caliper part on the finger side (7) has these stiffness terms:

$$k_{7,1}(i,j) = 0, \quad k_{7,2}(i,j) = -\sum_{p=1}^{2}\sum_{q=1}^{7}[k_{27pq}\phi_2(i,a_{27pg})\phi_2(j,a_{27pq})], \tag{A.28}$$

$$k_{7,3}(i,j) = 0, \quad k_{7,p}(i,j) = 0 \ \text{ for } p = 4,5, \tag{A.29}$$

$$k_{7,6}(i,j) = -\sum_{p=1}^{2} k_{6gp}\phi_6(i,a_{6gp})\phi_6(j,a_{6gp}) \tag{A.30}$$

and

$$k_{7,7}(i,j) = \sum_{p=1}^{2} k_{67p}\phi_6(i,a_{67p})\phi_7(j,a_{67p}). \tag{A.31}$$

APPENDIX B. SYSTEM PARAMETERS

The following lists of physical and geometrical properties are stated in SI units:

$EI_1 = 8{\cdot}994 \times 10^4$	stiffness of disc
$EI_p = 1{\cdot}179 \times 10^3$	stiffness of pads, $p = 2,3$
$h = 0{\cdot}045$	thickness of disc
$k_l = 1{\cdot}215 \times 10^{10}$	lining stiffness
$l = 0{\cdot}250$	length of pad
$L = 1{\cdot}301$	disc equivalent length
$m_1 = 30{\cdot}32$	disc mass per unit length
$m_p = 7{\cdot}873$	pad mass per unit length, $p = 2,3$
$N_0 = 1{\cdot}0 \times 10^5$	normal force per unit length
$\mu = 0{\cdot}35$	coefficient of friction

Stiffness and location of discrete springs:

$$\left.\begin{matrix} k_{271q} \\ k_{272q} \\ k_{34q} \\ k_{35q} \end{matrix}\right\} = 4{\cdot}09 \times \begin{cases} 10^9 \\ 10^{10} \\ 10^{11} \\ 10^{12} \\ 10^{11} \\ 10^{10} \\ 10^9 \end{cases} \text{pad}-\text{caliper contact stiffness}$$

$$-a_{271q} = a_{272q} = \begin{cases} 0{\cdot}0325 \\ 0{\cdot}0417 \\ 0{\cdot}0508 \\ 0{\cdot}0600 \\ 0{\cdot}0692 \\ 0{\cdot}0783 \\ 0{\cdot}0875 \end{cases} \text{location of pad}-\text{caliper contact}$$

$$-a_{34q} = a_{35q} = \begin{cases} 0{\cdot}0825 \\ 0{\cdot}0733 \\ 0{\cdot}0642 \\ 0{\cdot}0550 \\ 0{\cdot}0458 \\ 0{\cdot}0367 \\ 0{\cdot}0275 \end{cases} \text{location of pad}-\text{piston contact}$$

$k_{2g1} = k_{3g1} = 4{\cdot}0 \times 10^8$	abutment contact stiffness
$a_{2g1} = a_{3g1} = 0{\cdot}125$	location of abutment contact
$k_{6g1} = k_{6g2} = 5{\cdot}0 \times 10^8$	caliper–ground stiffness
$-a_{6g1} = a_{6g1} = 0{\cdot}15$	location of caliper–ground contact
$k_{671} = k_{672} = 2{\cdot}34 \times 10^8$	stiffness of caliper–caliper connection
$-a_{671} = a_{672} = 0{\cdot}16$	location of caliper–caliper connection